INTERNATIONAL JOURNAL FOR NUMERICAL METHODS IN FLUIDS
Int. J. Numer. Meth. Fluids 2006; **50**:1063–1084
Published online 9 November 2005 in Wiley InterScience (www.interscience.wiley.com). DOI: 10.1002/fld.1110

Extension of a high-resolution scheme to 1D liquid–gas flow

J. R. García-Cascales[1,*,†] and J. M. Corberán-Salvador[2,‡]

[1] *UPCT, Departamento de Ingeniería Térmica y de Fluidos, Dr. Fleming, 30203 Cartagena, Murcia, Spain*
[2] *UPV, Departamento de Termodinámica Aplicada, Camino de Vera, s/n, 40000 Valencia, Spain*

SUMMARY

This paper presents the extension of a high-resolution conservative scheme to the one-dimensional one-pressure six-equation two-fluid flow model. Only mixtures of water and air have been considered in this study, both fluids have been characterized using simple equations of state, namely stiffened gas for the liquid phase and perfect gas for the gas phase. The resulting scheme is explicit and first-order accurate in space and time. A second-order version of the scheme has also been derived using the MUSCL strategy and slope limiters. Some numerical results show the good capabilities of this type of schemes in the solution of discontinuities in two-fluid flow problems, all of them are based on water/air numerical benchmarks widely used in the two-phase flow literature. Copyright © 2005 John Wiley & Sons, Ltd.

KEY WORDS: Two-phase flow; two-fluid flow; hyperbolic systems

1. INTRODUCTION

During the last decades and due to the great amount of industrial applications where multiphase flow can be found, many codes have been developed in order to analyse different problems. Special interest appeared in the nuclear industry to prevent and analyse different accidents, mainly loss of coolant accidents. Such codes have resulted to be very robust and able to deal with a wide regime of fluids and conditions, for instance TRAC [1], RELAP [2] and CATHARE [3].

Their weaknesses in the treatment of strong discontinuities accompanying strong compressibility effects have led many researchers to develop a new generation of codes based on the extension to the solution of two-phase flow problems of well-known numerical schemes whose suitable characteristics had already been proved in the solution of a great variety of

*Correspondence to: J. R. García-Cascales, UPCT, Departamento de Ingeniería Térmica y de Fluidos, Dr. Fleming, 30203 Cartagena, Murcia, Spain.
†E-mail: jr.garcia@upct.es
‡E-mail: corberan@ter.upv.es

Received 20 April 2005
Revised 27 July 2005
Accepted 22 August 2005

single-phase problems at all flow speeds. Many of them are based on the exact or approximate solution of the Riemann problem using Godunov-like methods such as approximate Riemann solvers or flux splitting methods. Pioneer works are [4, 5]. Among the most recent contributions stand out the volumes finis à flux caractéristiques (VFFC) scheme [6], Toumi's approximate Riemann solver [7], Städtke's flux vector splitting scheme [8, 9], Masella's Godunov method [10, 11], Bedjaoui and Sainsaulieu's models for stratified two-phase flow [12, 13], the application of Godunov-type schemes by Berger and Colombeau [14], the non-conservative models of Tiselj and Petelin [15], the Hwang's one [16], the Sung-Jae Lee's flux vector splitting scheme [17, 18] and the extension of the AUSM schemes to two-fluid flows [19].

Such extensions have not been an easy task to do mainly because of the non-hyperbolic character of the two-phase flow system of equations. Many researchers have solved this problem by adding some regularising terms, often virtual mass terms or pressure correction terms, which provide the necessary hyperbolicity to the problem (see Reference [20]). Other problems such as stiff source terms and complex equations of state have had to be overcome and their correct treatment is still a challenge to researchers.

Our contribution is focused on the extension of an advanced conservative and explicit scheme defined as

$$W_j^{n+1} = W_j^n - \frac{\Delta t}{\Delta x}[F_{j+\frac{1}{2}} - F_{j-\frac{1}{2}}] + \Delta t S_j^n \tag{1}$$

to obtain approximate solutions of the system of equations in one-dimensional, one-pressure two-fluid flow. In particular, it is a TVD scheme traditionally applied to non-viscous single-phase compressible flows. Alternatively to the schemes that use the non-conservative form of the equations, we will transform the system into a conservative set of equations by means of the inclusion of non-conservative terms in the source term. This is one of the main ideas on which our work is based. This idea has also been put into practice in other interesting works such as References [21, 22] or [19], where Boltzman-type schemes in the first and AUSM+ schemes in the second have been successfully extended to two-fluid flows.

The system of equations that governs one-dimensional two-fluid flow is introduced in the first sections. The closure relationships and the equations of state—that characterize the thermodynamic behaviour of the fluids—are also presented. Then, we will focus our attention on the presentation of the eigenstructure of the system. We will introduce the TVD scheme and the proposed extension to two-phase flow. The work is completed with some numerical results and with some final conclusions.

2. ON THE SYSTEM OF EQUATIONS IN 1D TWO-PHASE FLOW

The unsteady one-pressure two-fluid flow model is characterized by a set of three balance equations—for mass, momentum and total energy—that for each phase yields the following system of equations:

$$\frac{\partial}{\partial t}(\alpha\rho_{\mathrm{v}}) + \frac{\partial}{\partial x}(\alpha\rho_{\mathrm{v}}u_{\mathrm{v}}) = \Gamma_{\mathrm{v}}$$

$$\frac{\partial}{\partial t}((1-\alpha)\rho_{\mathrm{l}}) + \frac{\partial}{\partial x}((1-\alpha)\rho_{\mathrm{l}}u_{\mathrm{l}}) = \Gamma_{\mathrm{l}}$$

$$\begin{gathered}
\frac{\partial}{\partial t}(\alpha\rho_{\mathrm{v}}u_{\mathrm{v}}) + \frac{\partial}{\partial x}(\alpha\rho_{\mathrm{v}}u_{\mathrm{v}}^2 + \alpha p) - p^{\mathrm{i}}\frac{\partial\alpha}{\partial x} = \alpha\rho_{\mathrm{v}}g + F_{\mathrm{v}}^{\mathrm{nv}} + \varphi_{\mathrm{v}} \\
\frac{\partial}{\partial t}((1-\alpha)\rho_{\mathrm{l}}u_{\mathrm{l}}) + \frac{\partial}{\partial x}((1-\alpha)\rho_{\mathrm{l}}u_{\mathrm{l}}^2 + (1-\alpha)p) + p^{\mathrm{i}}\frac{\partial\alpha}{\partial x} = (1-\alpha)\rho_{\mathrm{l}}g + F_{\mathrm{l}}^{\mathrm{nv}} + \varphi_{\mathrm{l}} \qquad (2) \\
\frac{\partial}{\partial t}(\alpha\rho_{\mathrm{v}}E_{\mathrm{v}}) + \frac{\partial}{\partial x}(\alpha\rho_{\mathrm{v}}H_{\mathrm{v}}u_{\mathrm{v}}) + p\frac{\partial\alpha}{\partial t} = \alpha\rho_{\mathrm{v}}gu_{\mathrm{v}} + \psi_{\mathrm{v}} \\
\frac{\partial}{\partial t}((1-\alpha)\rho_{\mathrm{l}}E_{\mathrm{l}}) + \frac{\partial}{\partial x}((1-\alpha)\rho_{\mathrm{l}}H_{\mathrm{l}}u_{\mathrm{l}}) - p\frac{\partial\alpha}{\partial t} = (1-\alpha)\rho_{\mathrm{l}}gu_{\mathrm{l}} + \psi_{\mathrm{l}}
\end{gathered}$$

where α is the void fraction, ρ_k the density of phase k, either liquid (l) or vapour (gas) (v), u_k the velocity, p the pressure, $E_k = e_k + (u_k^2/2)$ is the specific total energy, with e_k its specific internal energy, $H_k = h_k + (u_k^2/2)$ is the specific total enthalpy of phase k with h_k its specific enthalpy, g is acceleration of gravity (9.81 m/s), p^{i} stands for the difference of pressure between each phase and the interface. As discussed previously, this term is included to make the system of equations hyperbolic, the approximation we will use is the one used in the CATHARE code [23]

$$p^{\mathrm{i}} = p - p_{\mathrm{i}} = \sigma\frac{\alpha(1-\alpha)\rho_{\mathrm{v}}\rho_{\mathrm{l}}}{\alpha\rho_{\mathrm{l}} + (1-\alpha)\rho_{\mathrm{v}}}(u_{\mathrm{v}} - u_{\mathrm{l}})^2$$

Γ_k is the net mass transfer flux through the interface, F_k^{nv} the non-viscous force, considers non-viscous friction effects between the phases.

φ_k and ψ_k gather the contributions other physical effects such as wall friction, interfacial transfer of momentum and energy, heat transfer through the walls, volume heat sources, etc. to the momentum and energy equations. However, in our study, we are not going to consider any source term other than gravity.

As commented above, we will restrict our study to water and air mixtures. Since we are more interested in the numerical performance of the scheme than in the perfect representation of the behaviour of the fluids, we have utilized simplified equations of state following other works such as References [24] or [19] (for the gas phase the perfect gas equation of state and for the liquid phase the so-called stiffened gas equation). Otherwise their validity is sufficient for a wide range of problems. Thus, we have considered the following expressions for densities in each case

$$\rho_{\mathrm{v}} = \frac{\gamma_{\mathrm{v}}p}{(\gamma_{\mathrm{v}}-1)h_{\mathrm{v}}} \quad \text{perfect gas}$$

$$\rho_{\mathrm{l}} = \frac{\gamma_{\mathrm{l}}(p - p_\infty)}{(\gamma_{\mathrm{l}}-1)h_{\mathrm{l}}} \quad \text{stiffened gas}$$

with $\gamma_{\mathrm{v}} = 1.4$, $c_{p\mathrm{v}} = 1008\,\mathrm{J/(kg\,K)}$, $\gamma_{\mathrm{l}} = 2.8$, $p_\infty = 8.5\times10^8\,\mathrm{Pa}$ and $c_{p\mathrm{l}} = 4186\,\mathrm{J/(kg\,K)}$. Enthalpy and speed of sound of phase k are given by $h_k = c_{pk}T_k$ and $c_k = ((\gamma_k - 1)c_{pk}T_k)^{1/2}$, respectively.

3. NUMERICAL SCHEME

In this section, we will study the extension of an upwind conservative scheme for single-phase flow to two-fluid flow. In its single-phase application the scheme is TVD, e.g. [25] or [26]. Despite the non-conservative character of the system of equations (2), we mean to extrapolate and extend such a scheme to the solution of two-fluid problems, expecting to inherit some benefit of the application of these TVD schemes, such as convergence and stability. For these schemes the property

$$\mathrm{TV}(w^{n+1}) \leqslant \mathrm{TV}(w^n) \quad \forall n$$

holds, where the total variation is defined by $\mathrm{TV}(w^n) = \sum_{i=-\infty}^{\infty} |w_{i+1}^n - w_i^n|$ and is expected not to increase in time. This is important as it guarantees convergence and the non-production of false oscillations.

3.1. First-order numerical scheme

To obtain approximate solutions of the system of equations (2) we propose the scheme given by

$$W_j^{n+1} = W_j^n - \frac{\Delta t}{\Delta x}[F_{j+\frac{1}{2}} - F_{j-\frac{1}{2}}] + \Delta t S_j^n$$

where the flux at the interface is defined by

$$F_{j+\frac{1}{2}} = \tfrac{1}{2}[F_{j+1} + F_j - P_{j+\frac{1}{2}} h(D_{j+\frac{1}{2}}) P_{j+\frac{1}{2}}^{-1}(F_{j+1} - F_j)]$$

where $D_{j+\frac{1}{2}}$ is the diagonal matrix of eigenvalues λ_i of the jacobian matrix J, defined in Equation (4) and evaluated in the point $x_{j+\frac{1}{2}}$. $P_{j+\frac{1}{2}}$ the matrix of right eigenvectors of J also evaluated at the intercell, $P_{j+\frac{1}{2}}^{-1}$ the matrix of left eigenvectors, inverse of the previous one, $h(D_{j+\frac{1}{2}}) = \mathrm{diag}(\mathrm{sign}(\lambda_1), \ldots, \mathrm{sign}(\lambda_6))$. Where 'sign' stands for the sign function given by

$$\mathrm{sign}(\lambda) = \begin{cases} 1 & \text{if } \lambda \geqslant 0 \\ -1 & \text{otherwise} \end{cases}$$

The definition of the numerical flux allows the introduction of the concept 'sign of a matrix'. In the case of the jacobian matrix, we define its sign as

$$\mathrm{sign}(J) = P h(D) P^{-1}$$

For its evaluation we will use the algorithm stated below which assumes that the eigenvalues of J are clustered in $[L_0, -1] \cup \{0\} \cup [1, L_0]$, instead of working out the eigenstructure of the system for every cell at each time step which will be very time consuming, and if

$$a_0 = \frac{1}{L_0(L_0 + 1)}$$

$$A_0 = A$$

then

$$A_{n+1} = P_{a_n}(A_{n+1})$$

$$L_{n+1} = \frac{2(a_n + 1)}{3}\sqrt{\frac{a_n + 1}{3a_n}}$$

$$a_{n+1} = \frac{1}{L_{n+1}(1 + L_{n+1})}$$

where the polynomial function P_a is defined by

$$P_a(X) = -aX^3 + (a + 1)X$$

The parameter L_0 has been chosen considering that the biggest eigenvalue is always lower than this

$$L_0 = \frac{(u_v + a_v)(u_l + a_l)}{(1 - \alpha)(u_v + a_v) + \alpha(u_l + a_l)}$$

This algorithm was developed in Reference [27], and has also been successfully employed by Ghidaglia *et al.* in the extension of their VFFC schemes to two-phase flow (see Reference [28] for example). The adoption of this method reduces the calculation time considerably as it has been verified in the calculations. It additionally avoids the complicated task of evaluating the eigenstructure of the flux vector, unlike other upwind schemes applied to two-fluid/phase flow problems such as other approximate Riemann solver [7] or other flux vector splitting methods [8].

3.2. Jacobian matrix of the system

In order to determine an expression for the numerical flux of our scheme we have chosen to write the system of Equations (2) in vector form as follows

$$W_t + F_x(W) = S(W) \tag{3}$$

where W is the vector of conserved variables, $F(W)$ is the physical flux vector and $S(W)$ groups the non-conservative terms and the other source terms, they are given by

$$W = \begin{bmatrix} \alpha\rho_v \\ (1 - \alpha)\rho_l \\ \alpha\rho_v u_v \\ (1 - \alpha)\rho_l u_l \\ \alpha\rho_v E_v \\ (1 - \alpha)\rho_l E_l \end{bmatrix} = \begin{bmatrix} w_1 \\ w_2 \\ w_3 \\ w_4 \\ w_5 \\ w_6 \end{bmatrix}$$

$$F(W)=\begin{bmatrix} \alpha\rho_{\mathrm{v}}u_{\mathrm{v}} \\ (1-\alpha)\rho_{\mathrm{l}}u_{\mathrm{l}} \\ \alpha\rho_{\mathrm{v}}u_{\mathrm{v}}^2+\alpha p \\ (1-\alpha)\rho_{\mathrm{l}}u_{\mathrm{l}}^2+(1-\alpha)p \\ \alpha\rho_{\mathrm{v}}H_{\mathrm{v}}u_{\mathrm{v}} \\ (1-\alpha)\rho_{\mathrm{l}}H_{\mathrm{l}}u_{\mathrm{l}} \end{bmatrix}=\begin{bmatrix} w_3 \\ w_4 \\ \dfrac{w_3^2}{w_1}+\alpha p \\ \dfrac{w_4^2}{w_2}+(1-\alpha)p \\ (w_5+\alpha p)\dfrac{w_3}{w_1} \\ (w_6+(1-\alpha)p)\dfrac{w_4}{w_2} \end{bmatrix}$$

$$S(W)=\begin{bmatrix} \Gamma_{\mathrm{v}} \\ \Gamma_{\mathrm{l}} \\ p^{\mathrm{i}}\dfrac{\partial\alpha}{\partial x}+\alpha\rho_{\mathrm{v}}g+F_{\mathrm{v}}^{\mathrm{nv}}+\varphi_{\mathrm{v}} \\ -p^{\mathrm{i}}\dfrac{\partial\alpha}{\partial x}+(1-\alpha)\rho_{\mathrm{l}}g+F_{\mathrm{l}}^{\mathrm{nv}}+\varphi_{\mathrm{l}} \\ -p^{\mathrm{i}}\dfrac{\partial\alpha}{\partial t}+\alpha\rho_{\mathrm{v}}gu_{\mathrm{v}}+\psi_{\mathrm{v}} \\ p^{\mathrm{i}}\dfrac{\partial\alpha}{\partial t}+(1-\alpha)\rho_{\mathrm{l}}gu_{\mathrm{l}}+\psi_{\mathrm{l}} \end{bmatrix}$$

For the above system (Equation (3)) the jacobian matrix of the physical flux $J(W)=\partial F(W)/\partial W$ is given by

$$J(W)=\begin{bmatrix} 0 & 0 \\ 0 & 0 \\ -u_{\mathrm{v}}^2+p\dfrac{\partial\alpha}{\partial w_1}+\alpha\dfrac{\partial p}{\partial w_1} & p\dfrac{\partial\alpha}{\partial w_2}+\alpha\dfrac{\partial p}{\partial w_2} \\ -p\dfrac{\partial\alpha}{\partial w_1}+(1-\alpha)\dfrac{\partial p}{\partial w_1} & -u_{\mathrm{l}}^2-p\dfrac{\partial\alpha}{\partial w_2}+(1-\alpha)\dfrac{\partial p}{\partial w_2} \\ -u_{\mathrm{v}}H_{\mathrm{v}}+u_{\mathrm{v}}\left(p\dfrac{\partial\alpha}{\partial w_1}+\alpha\dfrac{\partial p}{\partial w_1}\right) & u_{\mathrm{v}}\left(p\dfrac{\partial\alpha}{\partial w_2}+\alpha\dfrac{\partial p}{\partial w_2}\right) \\ u_{\mathrm{l}}\left(-p\dfrac{\partial\alpha}{\partial w_1}+(1-\alpha)\dfrac{\partial p}{\partial w_1}\right) & -H_{\mathrm{l}}u_{\mathrm{l}}+u_{\mathrm{l}}\left(-p\dfrac{\partial\alpha}{\partial w_2}+(1-\alpha)\dfrac{\partial p}{\partial w_2}\right) \end{bmatrix}$$

$$
\begin{bmatrix}
1 & 0 \\
0 & 1 \\
2u_v + p\dfrac{\partial\alpha}{\partial w_3} + \alpha\dfrac{\partial p}{\partial w_3} & p\dfrac{\partial\alpha}{\partial w_4} + \alpha\dfrac{\partial p}{\partial w_4} \\
-p\dfrac{\partial\alpha}{\partial w_3} + (1-\alpha)\dfrac{\partial p}{\partial w_3} & 2u_l - p\dfrac{\partial\alpha}{\partial w_4} + (1-\alpha)\dfrac{\partial p}{\partial w_4} \\
H_v + u_v\left(p\dfrac{\partial\alpha}{\partial w_3} + \alpha\dfrac{\partial p}{\partial w_3}\right) & u_v\left(p\dfrac{\partial\alpha}{\partial w_4} + \alpha\dfrac{\partial p}{\partial w_4}\right) \\
u_l\left(-p\dfrac{\partial\alpha}{\partial w_3} + (1-\alpha)\dfrac{\partial p}{\partial w_3}\right) & H_l + u_l\left(-p\dfrac{\partial\alpha}{\partial w_4} + (1-\alpha)\dfrac{\partial p}{\partial w_4}\right) \\
0 & 0 \\
0 & 0 \\
p\dfrac{\partial\alpha}{\partial w_5} + \alpha\dfrac{\partial p}{\partial w_5} & p\dfrac{\partial\alpha}{\partial w_6} + \alpha\dfrac{\partial p}{\partial w_6} \\
-p\dfrac{\partial\alpha}{\partial w_5} + (1-\alpha)\dfrac{\partial p}{\partial w_5} & -p\dfrac{\partial\alpha}{\partial w_6} + (1-\alpha)\dfrac{\partial p}{\partial w_6} \\
u_v\left(1 + p\dfrac{\partial\alpha}{\partial w_5} + \alpha\dfrac{\partial p}{\partial w_5}\right) & u_v\left(p\dfrac{\partial\alpha}{\partial w_6} + \alpha\dfrac{\partial p}{\partial w_6}\right) \\
u_l\left(-p\dfrac{\partial\alpha}{\partial w_5} + (1-\alpha)\dfrac{\partial p}{\partial w_5}\right) & u_l\left(1 - p\dfrac{\partial\alpha}{\partial w_6} + (1-\alpha)\dfrac{\partial p}{\partial w_6}\right)
\end{bmatrix} \tag{4}
$$

The derivatives of pressure and void fraction with respect to the conserved variables, can be obtained from the derivatives of the conserved variables with respect to the primitive variables $\partial W/\partial V$, through the following inversion:

$$\frac{\partial V}{\partial W} = \left(\frac{\partial W}{\partial V}\right)^{-1}$$

where, if the primitive variables are $V = (\alpha, u_v, u_l, p, h_v, h_l)^t$

$$
\frac{\partial W}{\partial V} = \begin{bmatrix}
\rho_v & 0 & 0 & \alpha\dfrac{\partial\rho_v}{\partial p} & \alpha\dfrac{\partial\rho_v}{\partial p} & 0 \\
-\rho_l & 0 & 0 & (1-\alpha)\dfrac{\partial\rho_l}{\partial p} & 0 & (1-\alpha)\dfrac{\partial\rho_l}{\partial h_l} \\
\rho_v u_v & \alpha\rho_v & 0 & \alpha u_v\dfrac{\partial\rho_v}{\partial p} & \alpha u_v\dfrac{\partial\rho_v}{\partial p} & 0 \\
-\rho_l u_l & 0 & (1-\alpha)\rho_l & (1-\alpha)u_l\dfrac{\partial\rho_l}{\partial p} & 0 & (1-\alpha)u_l\dfrac{\partial\rho_l}{\partial h_l} \\
\rho_v(H_v - p) & \alpha\rho_v u_v & 0 & \alpha H_v\dfrac{\partial\rho_v}{\partial p} - \alpha & \alpha H_v\dfrac{\partial\rho_v}{\partial p} + \alpha\rho_v & 0 \\
-\rho_l(H_l - p) & 0 & (1-\alpha)\rho_l u_l & (1-\alpha)H_l\dfrac{\partial\rho_l}{\partial p} - (1-\alpha) & 0 & (1-\alpha)H_l\dfrac{\partial\rho_l}{\partial h_l} + (1-\alpha)\rho_l
\end{bmatrix}
$$

and finally

$$\frac{\partial\alpha}{\partial w_1} = \frac{(1-\alpha)}{d}\rho_\mathrm{l} c_\mathrm{l}^{-2}\left(\rho_\mathrm{v} + \frac{\partial\rho_\mathrm{v}}{\partial h_\mathrm{v}}(H_\mathrm{v} - u_\mathrm{v}^2)\right)$$

$$\frac{\partial\alpha}{\partial w_2} = -\frac{\alpha}{d}\rho_\mathrm{v} c_\mathrm{v}^{-2}\left(\rho_\mathrm{l} + \frac{\partial\rho_\mathrm{l}}{\partial h_\mathrm{l}}(H_\mathrm{l} - u_\mathrm{l}^2)\right)$$

$$\frac{\partial\alpha}{\partial w_3} = \frac{(1-\alpha)}{d}\rho_\mathrm{l} u_\mathrm{v} c_\mathrm{l}^{-2}\frac{\partial\rho_\mathrm{v}}{\partial h_\mathrm{v}}$$

$$\frac{\partial\alpha}{\partial w_4} = -\frac{\alpha}{d}\rho_\mathrm{v} u_\mathrm{l} c_\mathrm{v}^{-2}\frac{\partial\rho_\mathrm{l}}{\partial h_\mathrm{l}}$$

$$\frac{\partial\alpha}{\partial w_5} = -\frac{(1-\alpha)}{d}\frac{\partial\rho_\mathrm{v}}{\partial h_\mathrm{v}}\rho_\mathrm{l} c_\mathrm{l}^{-2}$$

$$\frac{\partial\alpha}{\partial w_6} = \frac{\alpha}{d}\frac{\partial\rho_\mathrm{l}}{\partial h_\mathrm{l}}\rho_\mathrm{v} c_\mathrm{v}^{-2}$$

and

$$\frac{\partial p}{\partial w_1} = \left(\frac{\partial\rho_\mathrm{l}}{\partial h_\mathrm{l}}p - \rho_\mathrm{l}^2\right)\left(\rho_\mathrm{v} + \frac{\partial\rho_\mathrm{v}}{\partial h_\mathrm{v}}(H_\mathrm{v} - u_\mathrm{v}^2)\right)\frac{1}{d}$$

$$\frac{\partial p}{\partial w_2} = \left(\frac{\partial\rho_\mathrm{v}}{\partial h_\mathrm{v}}p - \rho_\mathrm{v}^2\right)\left(\rho_\mathrm{l} + \frac{\partial\rho_\mathrm{l}}{\partial h_\mathrm{l}}(H_\mathrm{l} - u_\mathrm{l}^2)\right)\frac{1}{d}$$

$$\frac{\partial p}{\partial w_3} = \frac{\partial\rho_\mathrm{v}}{\partial h_\mathrm{v}}\left(\frac{\partial\rho_\mathrm{l}}{\partial h_\mathrm{l}}p - \rho_\mathrm{l}^2\right)u_\mathrm{v}\frac{1}{d}$$

$$\frac{\partial p}{\partial w_4} = \frac{\partial\rho_\mathrm{l}}{\partial h_\mathrm{l}}\left(\frac{\partial\rho_\mathrm{v}}{\partial h_\mathrm{v}}p - \rho_\mathrm{v}^2\right)u_\mathrm{l}\frac{1}{d}$$

$$\frac{\partial p}{\partial w_5} = \frac{\partial\rho_\mathrm{v}}{\partial h_\mathrm{v}}\left(\frac{\partial\rho_\mathrm{l}}{\partial h_\mathrm{l}}p - \rho_\mathrm{l}^2\right)\frac{1}{d}$$

$$\frac{\partial p}{\partial w_6} = \frac{\partial\rho_\mathrm{l}}{\partial h_\mathrm{l}}\left(\frac{\partial\rho_\mathrm{v}}{\partial h_\mathrm{v}}p - \rho_\mathrm{v}^2\right)\frac{1}{d}$$

where

$$d = \frac{\partial\rho_\mathrm{l}}{\partial h_\mathrm{l}}\left[\frac{\partial\rho_\mathrm{v}}{\partial h_\mathrm{v}}p + \rho_\mathrm{v}\left(\alpha p\frac{\partial\rho_\mathrm{v}}{\partial p} + (1-\alpha)\rho_\mathrm{v}\right)\right] + \rho_\mathrm{l}\left[\alpha\rho_\mathrm{l}\rho_\mathrm{v} c_\mathrm{v}^{-2} - (1-\alpha)\frac{\partial\rho_\mathrm{l}}{\partial p}\left(\frac{\partial\rho_\mathrm{v}}{\partial h_\mathrm{v}}p + \rho_\mathrm{v}^2\right)\right]$$

with the speeds of sound of each phase given by

$$c_k^2 = \frac{1}{\dfrac{\partial\rho_k}{\partial p} + \dfrac{1}{\rho_k}\dfrac{\partial\rho_k}{\partial h_k}} \tag{5}$$

Our simple equations of state yield the following derivatives:

$$\frac{\partial \rho_v}{\partial p} = \frac{\rho_v}{p}, \quad \frac{\partial \rho_v}{\partial h_v} = -\frac{\rho_v}{h_v}$$

$$\frac{\partial \rho_l}{\partial p} = \frac{\rho_v}{p + p_\infty}, \quad \frac{\partial \rho_l}{\partial h_l} = -\frac{\rho_l}{h_l}$$

which substituted in Equation (5) gives the following speeds of sound for each phase

$$c_v = ((\gamma_v - 1)c_{pv}T_v)^{1/2} \quad c_l = ((\gamma_l - 1)c_{pl}T_l)^{1/2}$$

3.3. Second-order numerical scheme

Although it is beyond the scope of this work, a second-order scheme is also possible, which can be accomplished by means of the MUSCL strategy. We could follow the formulation of Hancock's method described in Reference [29]:

1. Data reconstruction, in which we adopt a linear approximation of the values of the primitive variables

$$V_j^L = V_j^n - \frac{1}{2}\Delta x \frac{\partial V}{\partial x}$$

$$V_j^R = V_j^n + \frac{1}{2}\Delta x \frac{\partial V}{\partial x}$$

   To avoid spurious oscillations the spatial derivatives of the primitives can be limited by using any of the limiters described in Reference [30]:

2. Time evolution of $\Delta t/2$ of W_j^L and W_j^R,

$$\bar{W}_j^{L,R} = W_j^{L,R} - \frac{\Delta t}{2\Delta x}[F(W_j^R) - F(W_j^L)]$$

3. Approximate solution of the piece-wise constant data Riemann problem,

$$w_t + F_x(W) + S(W) = 0$$

$$W(x,0) = \begin{cases} \bar{W}_j^R & \text{if } x < 0 \\ \bar{W}_{j+1}^L & \text{if } x > 0 \end{cases}$$

   In this step we will use our approximate TVD flux in order to determine the numerical flux in the middle

$$F_{j+1/2} = F^{TVD}(\bar{W}_j^R, \bar{W}_{j+1}^L)$$

3.4. Time discretization

In the case of single-phase or two-phase homogeneous flow, the scheme is first order and TVD under the CFL condition

$$\frac{\Delta t}{\Delta x}\max|\mu^k| \leqslant 1$$

In our case we have chosen the time step defined in Reference [19], based on a volume fraction weighted average of acoustic-type signals. As in this case, we do not know the eigenstructure of the scheme and therefore the largest eigenvalue

$$\Delta t = \mathrm{CFL}\times\min_j\left[\frac{(1-\alpha)\Delta x}{|(u_\mathrm{l})_j|+(c_\mathrm{l})_j}+\frac{\alpha\Delta x}{|(u_\mathrm{v})_j|+(c_\mathrm{v})_j}\right]$$

where CFL is a CFL-like number which has been adjusted depending on the test. It has ranged from 0.1 to 0.9.

3.5. Discretization of source terms

The source term has been discretized using the following approximations:

- Spatial derivatives of the void fraction using a central or backward discretization depending on the case

$$\left(p\frac{\partial\alpha}{\partial x}\right)_j^n \simeq p_j\frac{\alpha_{j+1}^n-\alpha_{j-1}^n}{2\Delta x} \quad \text{and} \quad \left(p\frac{\partial\alpha}{\partial x}\right)_j^n \simeq p_j\frac{\alpha_j^n-\alpha_{j-1}^n}{\Delta x}$$

  We have used the centred approximation for most of the cases, which has yielded very good results. In the case of the water faucet test, which is presented in the following section, we have had to use a backward approximation. The influence of the source term discretization on the results merits a deeper study that will be left for future contributions. The upwinding of the space derivatives of void fraction and the other source terms could be a solution to this problem. Applications of such techniques to single-phase problems which might be extrapolated to two-phase flow problems can be found in Reference [31] for instance.
- Time derivatives of void fraction by means of a backward discretization in time leaving the scheme explicit

$$\left(p\frac{\partial\alpha}{\partial t}\right)_j^n \simeq p_j\frac{\alpha_j^n-\alpha_j^{n-1}}{\Delta t^{n-1}}$$

- Gravity terms as

$$(\alpha_k\rho_k g)_j^n \simeq (\alpha_k)_j^n(\rho_k)_j^n g$$

$$(\alpha_k\rho_k u_k g)_j^n \simeq (\alpha_k)_j^n(\rho_k u_k)_j^n g$$

- Non-viscous friction terms as

$$(F_\mathrm{v}^\mathrm{nv})_j^n \simeq -\frac{3}{8}\frac{C_\mathrm{d}}{R_\mathrm{b}}(\alpha)_j^n(\rho_\mathrm{l})_j^n|(u_\mathrm{v})_j^n-(u_\mathrm{l})_j^n|((u_\mathrm{v})_j^n-(u_{\mathrm{l}j})_j^n)$$

3.6. Some comments on boundary conditions and the model for phase appearance and disappearance

With regards to the boundary conditions we have followed the criteria chosen in Reference [19], so that the ghost cell approach has been used, where inlet and outlet states have been approximated by two fictitious cells whose states are a combination of imposed and extrapolated values. Considering primitive variables, at the inlet we have imposed all variables but pressure, while at the outlet, discharge pressure is usually the chosen variable to be imposed (as in the water faucet test). In the case of walls (tube ends in the 1D problems considered), we have considered mirror conditions in which all the variables coincide with the values of the adjacent cell, except for velocities that have different signs in order to guarantee that fluxes cancel each other out.

In the case of the model for phase appearance and disappearance ($\alpha\approx 0$ or $\alpha\approx 1$) we have also followed Reference [19] where some diffusion is added in order to avoid oscillations. The interested reader is referred to Reference [19].

4. NUMERICAL RESULTS

In this section, we are going to analyse the behaviour of the proposed scheme under certain numerical benchmarks. As commented above, we will only deal with mixtures of water and air. The tests that we have considered in this study are:

- Water faucet
- Shock tube
- Phase separation

4.1. Water faucet test

This test was proposed by Ramson (Numerical Bench. Test 2.1) [32]. It consists of a homogeneous mixture of water and air flowing downwards through a vertical pipe, (12 m long) under the action of gravity. A schematic of the transient taking place is shown in Figure 1.

This test case will allow us to analyse the stability of the scheme, its accuracy and the numerical diffusion it may produce. This test also shows the performance of the scheme when simple gravity effects are included in the system of equations and its ability to deal with a situation in which phases are mechanically decoupled.

Initial conditions are given by a void fraction, $\alpha = 0.2$, the phase velocities, $u_v = 0$ and $u_l = 10\,\mathrm{m/s}$, pressure, $p = 10^5\,\mathrm{Pa}$ and the phase temperatures $T_v = T_l = 50^\circ\mathrm{C}$. On the other hand, boundary conditions are characterized by the following inlet values: $\alpha_l = 0.8$, the phase velocities, $u_v = 0$ and $u_l = 10\,\mathrm{m/s}$ and the phase temperatures are $T_v = T_l = 50^\circ\mathrm{C}$. Outlet is characterized by a discharge pressure of $10^5\,\mathrm{Pa}$.

An analytical solution can be obtained neglecting the spatial variations of pressure in system (2), it is given by

$$\alpha = 1 - \frac{(1-\alpha_0)u_0}{\sqrt{u_0^2 + 2g(x-x_0)}}$$

for $x < (g/2)^2 + u_0 t$ and 0.2 otherwise (for a detailed analysis see Reference [33] for instance).

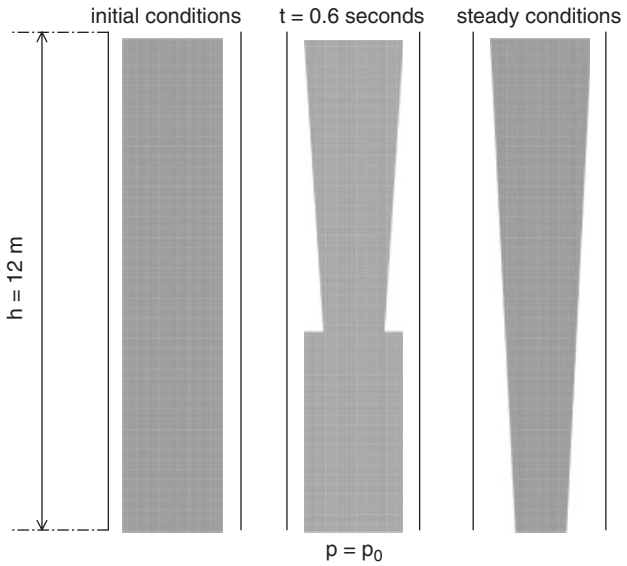

Figure 1. Scheme of the water faucet test.

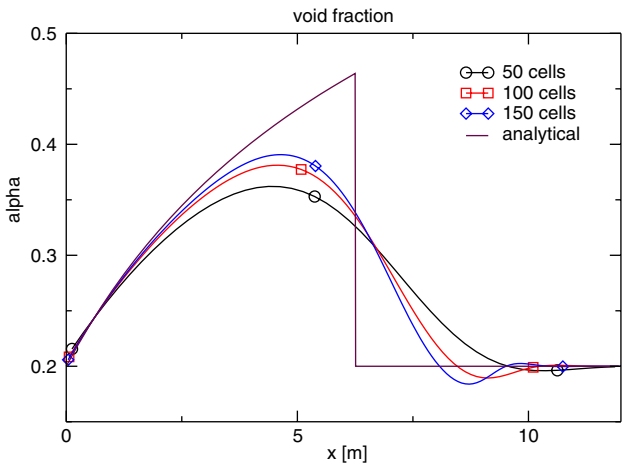

Figure 2. Void fraction at $t = 0.5$ for different number of cells.

To check the convergence and the stability character of the scheme, we have performed several computations using different discretizations. The corresponding results for different number of cells are shown in Figure 2, which have also been compared with the analytical solution at time $t = 0.5$ s. Despite that the front is sharper as the number of cells increases, some dissipation after the discontinuity also appears. As can be observed, void fraction presents a false numerical oscillation at the right-hand side of the solution leading to a non-bounded solution

and a loss of the monotonicity. Other numerical schemes have shown this behaviour in their initial developments (see Reference [34] or [35]) although these problems were solved by considering the six equation model [36] or by modifying the artificial terms that add hyperbolicity to the system of equations [35]. In our case, as we stated above, we have obtained the results displayed in Figure 2 by using a backward discretization in the approximation of the spatial derivative of void fraction. We have considered that it is not worthwhile to include the results corresponding to the central discretization since they are truly oscillatory. We think that the upwinding of the source terms might contribute to the improvement of these results and to reduce the overshoot found in the void fraction distribution when the mesh is refined.

To illustrate the results provided by this numerical scheme, we have collected the results corresponding to some of the most important variables (Figure 3), namely, void fraction, pressure, gas velocity and liquid velocity. Each one displays the solution at times $t = 0.5$ s and $t = 1.6$ (almost steady state). Void fraction results (first picture of Figure 3) have also been compared with the analytical solution at the steady state. We have observed that the numerical and analytical results match quite well, and no oscillation occurs at steady state. For this problem we have considered a value of CFL $= 0.9$ and an interfacial pressure correction parameter $\sigma = 3$.

Previous results are completed with the evolution of void fraction along the conduct. In Figure 4 we show the results corresponding to a mesh of 100 cells at different instants ($t = 0.1, 0.4, 0.6, 0.8$ and 1.2 s). The CFL-like parameter and the interfacial pressure correction parameter, σ, have been set to 0.9 and 3, respectively. Despite the small oscillations near the void fraction discontinuity, these results are quite similar to those reported by other researchers [24, 34–36].

4.2. Toumi's shock tube test

This test was proposed by Toumi [36]. In a 10 m long horizontal tube we place two mixtures of water and air separated by a membrane which are characterized by the following initial conditions: left state, $\alpha^{\mathrm{L}} = 0.25$ and $p^{\mathrm{L}} = 20$ MPa and right state $\alpha^{\mathrm{R}} = 0.1$ and $p^{\mathrm{R}} = 10$ MPa. Fluid temperatures are constant in both sides and equal to 35°C. Finally, this test differs from the original version proposed by Toumi in which both phase velocities are set at zero.

This benchmark allows us to study the behaviour of the scheme analysing strong shock waves. As there is no exact solution to this problem, we will compare our results with the ones provided by other researchers such as Toumi [37] or Tiselj [38].

In Figures 5 and 6 the results correspondi ng to different number of integration cells are shown.

The convergence to the exact solution as the number of cells increases can be observed. In the case of the liquid velocity, an oscillation appears as the grid is finer—near $x = 5$. Although there is no analytical solution of this problem and there exist certain discrepancy among the results reported by different authors respect to this test, from the comparison with other researchers' results can be concluded that the numerical scheme provides results quite similar to those shown in Paillère *et al.* [19], Toumi's [36] or Tiselj and Petelin's works [38]. In fact, they are much closer to the conservative formulation of Tiselj and Petelin's numerical scheme [38]. Calculations have been done with CFL $= 0.1$ and $\sigma = 3.0$ for different number of cells, higher CFL values do not allow to reach a stable solution which shows clearly certain CFL dependence.

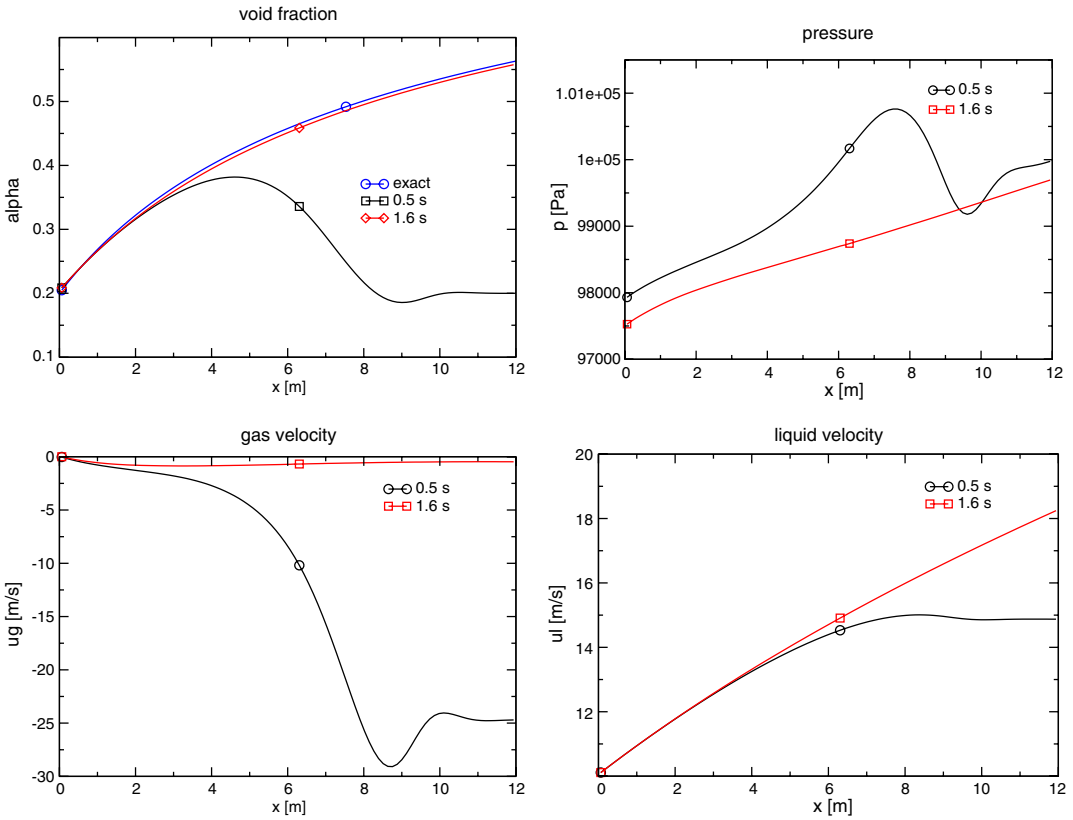

Figure 3. Water faucet test, distribution of some characteristic variables. From top to bottom, left to right, void fraction, pressure, gas velocity and liquid velocity.

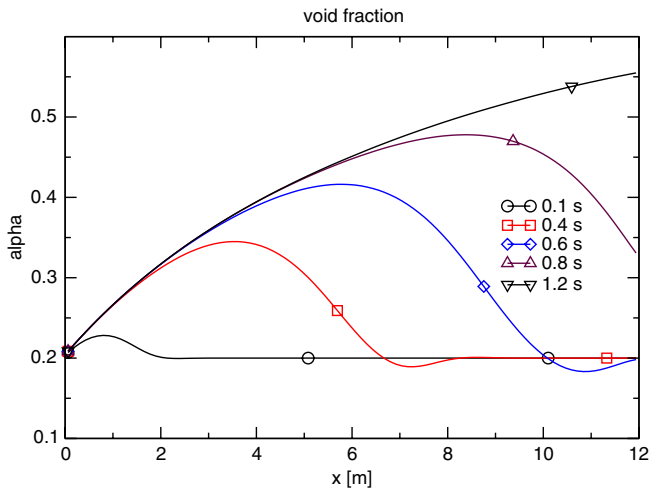

Figure 4. Water faucet test, distribution of void fraction at different instants ($t = 0.1, 0.4, 0.6, 0.8$ and 1.2 s).

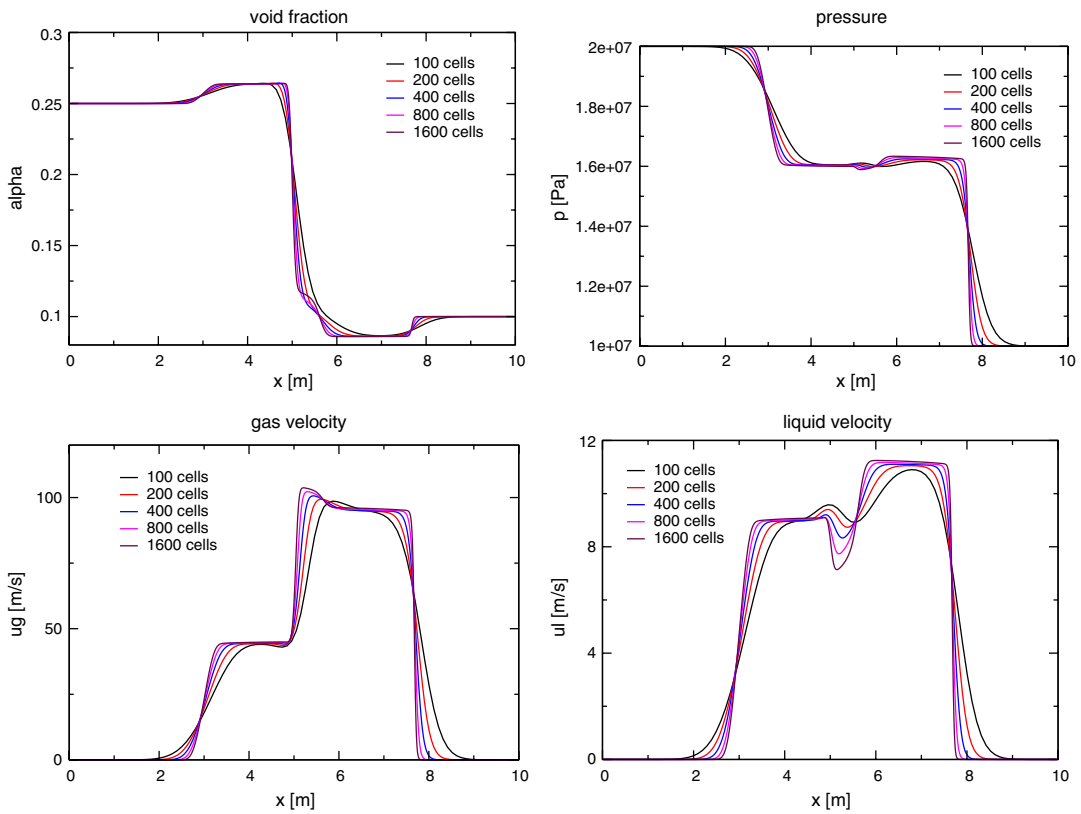

Figure 5. Toumi's shock tube, grid convergence study with the TVD scheme, $\sigma = 3.0$. From top to bottom, left to right, void fraction, pressure, gas velocity and liquid velocity.

As studied above, the interfacial pressure correction term affects the eigenstructure of the system and is characterized by the value of the parameter σ. In Figure 7 we show such an influence on the gas velocity and temperature for several values of σ. Small changes can be appreciated but, as commented in Reference [38], the effect in the solution of this sort of terms—pressure correction terms or adapted virtual mass terms to get hyperbolicity—is negligible when problems involving heat transfer, friction or interfacial phenomena are studied.

In this way, we will consider that values of $\sigma = 2$ or 3 provide enough hyperbolicity to the scheme and yield fairly good results [19].

4.3. Phase separation test

This test consists of a 7.5 m vertical tube filled with a two-fluid homogeneous mixture of water and air characterized by a void fraction of $\alpha = 0.5$, The mixture is separated under the action of gravity which takes place a sedimentation process. Here we will analyse a variation of the benchmark proposed by Young (Numerical Benchmark Test 2.4) [32] which has been used for the validation of numerical schemes such as those proposed by Städke [8]

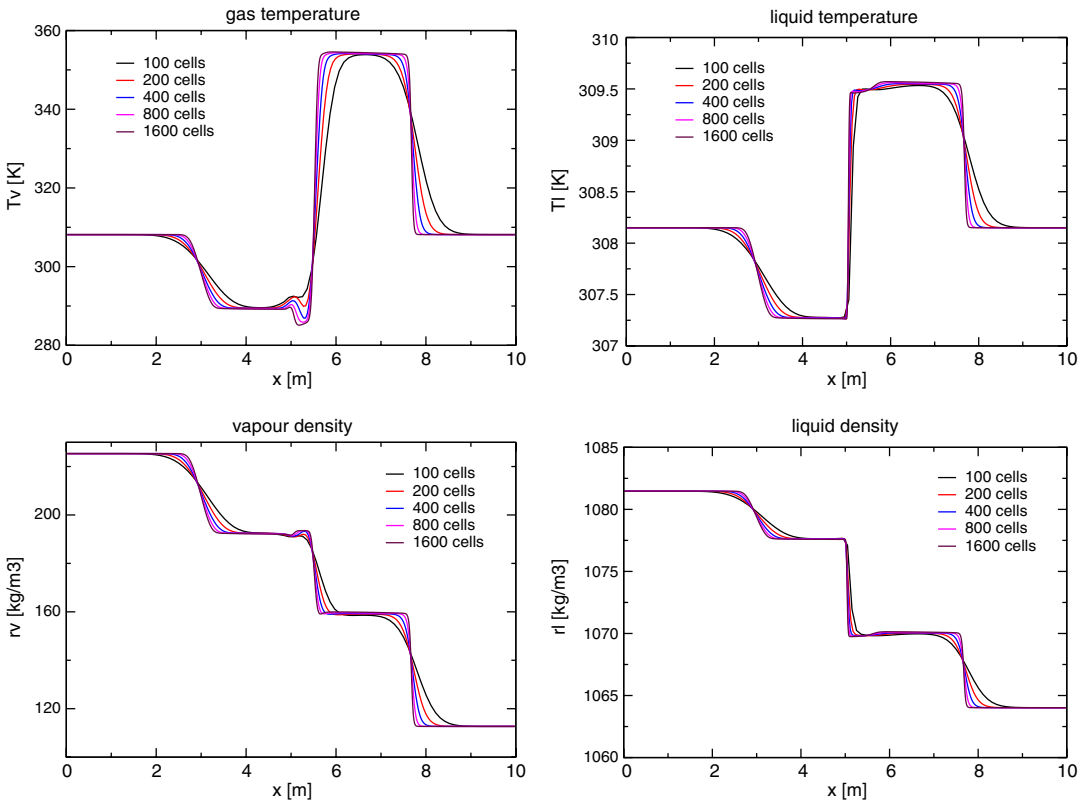

Figure 6. Toumi's shock tube, grid convergence study for $\sigma = 3.0$. From top to bottom, left to right, gas temperature, liquid temperature, gas density and liquid density.

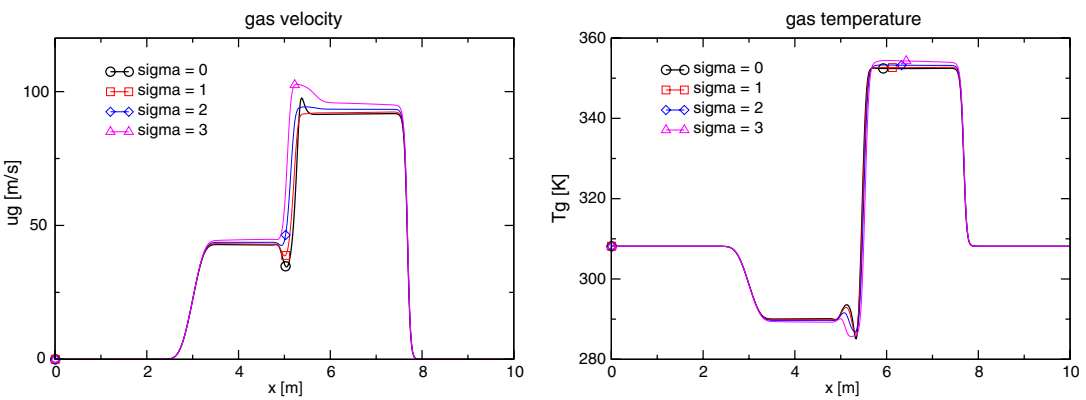

Figure 7. Effect of interfacial pressure correction term on the structure of the solution in the shock tube problem.

or Coquel *et al.* [21]. A schematic of the initial and steady-state conditions is represented in Figure 8.

This test allows us to evaluate the capability of the scheme to compute the propagation of void and pressure waves along the whole range of void fraction [0, 1] and allows us to test the phase disappearance algorithm. The code also faces other difficulties such as counter-current flow, low Mach number flow, and sharp interfaces.

In this case, we have considered the following initial conditions: $\alpha = 0.5$, $u_v = u_l = 0\,\mathrm{m/s}$, $p = 0.1\,\mathrm{MPa}$ and $T_v = T_l = 50^\circ\mathrm{C}$. Boundary conditions are mirror conditions both at the top and at the bottom.

The expected steady-state solution is characterized by a constant void fraction at each part of the tube, $\alpha = 0$ in the liquid side and $\alpha = 1$ in the vapour side. With respect to the pressure we will have practically constant pressure in the vapour side and a hydrostatic distribution of this variable in the liquid side. This has been depicted in Figure 9.

In Figure 10 we show the results produced by the TVD scheme. As can be observed, the calculated steady-state solution is near the analytical solution shown in Figure 9 although we have had to decrease the CFL number to obtain a good solution of the problem as in the shock tube test (about 0.1, certain CFL dependence is also noticed in this case). To illustrate the results we have also depicted the evolution of the void fraction profile (Figure 11), which clearly shows the upward and downward directed void fraction front. By reducing the CFL we are able to the reach steady state with greater accuracy. All the figures show a slightly oscillatory behaviour near the discontinuity between the states $\alpha = 0$ and 1. They are related to the appearance and disappearance of the phase. Additional studies are being carried out by the authors in this sense. It is believed that the combination of a three-equation model with the six-equation model used here when a phase is appearing or disappearing

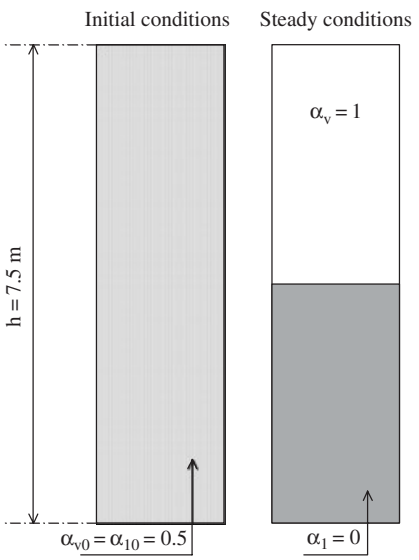

Figure 8. Scheme of the phase separation test.

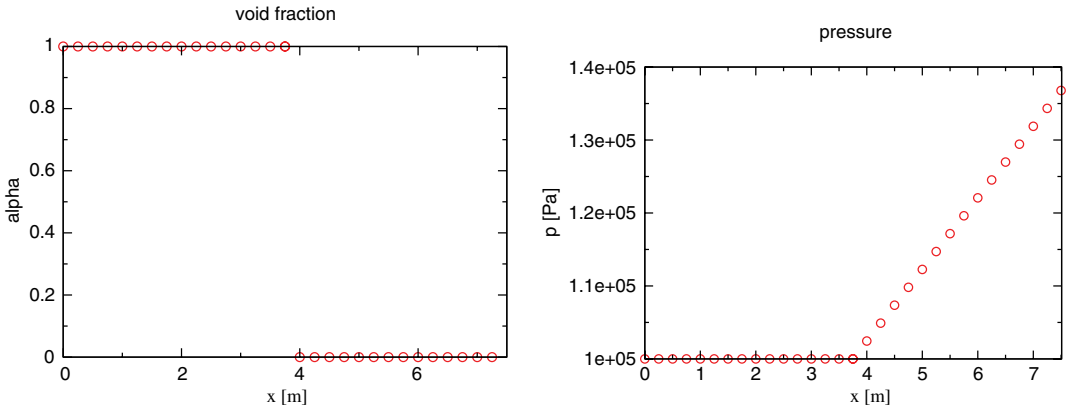

Figure 9. Phase separation test: steady-state solution for void fraction (left) and pressure (right).

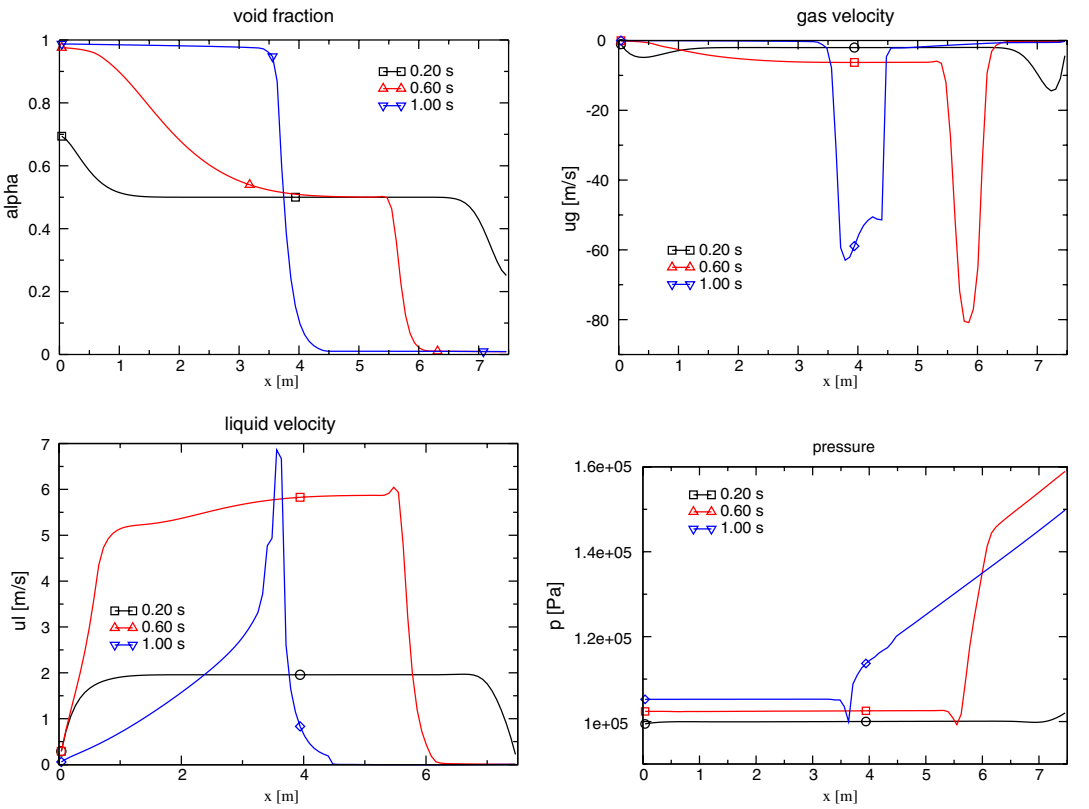

Figure 10. Phase separation test, first-order TVD. $\sigma = 2.0$ and CFL $= 0.1$. From top to bottom, left to right, void fraction, gas velocity, liquid velocity, pressure.

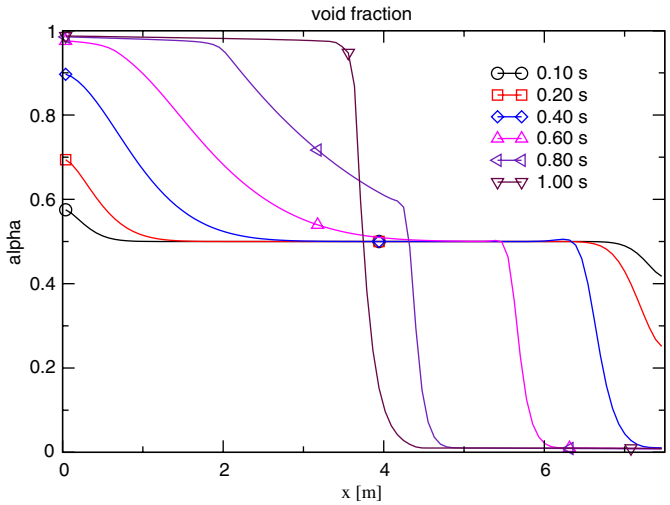

Figure 11. Evolution of void fraction for the phase separation test.

can be a possible solution to these cumbersome oscillations. Similar behaviour can be found for another very robust scheme such as the AUSM+ scheme extended to two-fluid flow in Reference [19].

5. CONCLUSIONS

In this paper, we have presented the extension of a high-resolution conservative scheme to the one-dimensional one-pressure six-equation two-fluid flow model. The scheme which is originally TVD in its single-phase application has behaved quite well in the solution of some known two-fluid flow numerical tests. We have encountered that the scheme is quite stable although some problems of accuracy have been found in the analysis of the water faucet test. The scheme has been able to handle simple gravity effects and situations in which phases have been mechanically decoupled. It has also characterized strong shocks waves fairly well. Typical problems found in the integration of this kind of numerical tests, among them, for instance the computation of the propagation of void and pressure waves along the whole range of void fraction $[0, 1]$, the analysis of counter-current flows, low Mach number flows and sharp interfaces have been overcome with success. The results shown in this work match quite well with those provided by other numerical schemes applied to the study of two-phase flow problems (see for example the recent work in Reference [39]).

We think that the developed scheme also offers advantages in solving more complex two-phase flow problems and future works will be focused on the extension of this approximate solver to problems with phase change in one and multiple dimensions. Different approaches for the discretization of the source terms—involving upwinding—should be studied as well.

NOMENCLATURE

α	void fraction
γ	specific heat ratio
λ	eigenvalue
ρ	density
σ	pressure correction parameter
∂	differential
Δ	increment
Γ	net mass transfer through the interface
ψ and ϕ	other source terms
c	speed of sound
c_p	specific heat at constant pressure
diag	diagonal matrix
e	specific internal energy
g	gravity ($9.81\,\mathrm{m/s^2}$)
h	specific enthalpy
p	pressure
p^{i}	pressure correction term
p_∞	correction term at the liquid equation of state
t	time
u	velocity
w	conserved variables
x	axial coordinate
C_{d}	drag coefficient
D	eigenvalues diagonal matrix
E_k	total internal energy
F_k^{nv}	non-viscous friction terms (drag force)
$F(W)$	flux vector
H	total enthalpy
J	jacobian matrix ($\partial F/\partial x$)
P	eigenvector matrix
R_{b}	bubble radius
$S(W)$	vector of source terms
T	temperature
V	vector of primitive variables
W	vector of conserved variables

Superscripts and subscripts

g or v	gas or vapour phase
i	interface
j	jth cell
k	a general phase
l	liquid
nv	non-viscous

t time derivative
x spatial derivative
L left
R right

ACKNOWLEDGEMENTS

We would like to thank to Ms. Emma C. Lumsden and Ms. Juana María Belchí at the UPCT for their help with the English.

REFERENCES

1. Borkowski JA, Wade NL. TRAC-BF1/MOD1 Models and correlations. *NUREG/CR-1391*, 1992.
2. Shieh AS, Ransom VH, Krishnamurthy R. Validation of numerical techniques in RELAP5/MOD3, *RELAP5/MOD3 Code Manual*, *NUREG/CR-5535*, 1994.
3. Barre F, Bernard M. The CATHARE code strategy and assessment. *Nuclear Engineering and Design* 1990; **124**:257–284.
4. Ransom VH, Hicks DL. Hyperbolic two pressure models for two phase flow. *Journal of Computational Physics* 1984; **53**:124–151.
5. Toro EF. Riemann-problem-based techniques for computing reactive two-phase flows. *Numerical Combustion*, Lectures Notes in Physics, 1989; 351.
6. Ghidaglia JM, Kumbaro A, Le Coq G. Une méthode volumenes finis a flux caractéristiques pour la résolution numérique des systemes hyperboliques de lois de consevation. *Comptes Rendus de l'Academic des Sciences*, *Paris* 1996; **322**(I):981–988.
7. Toumi I. A weak formulation of Roe's approximate Riemann solver. *Journal of Computational Physics* 1992; **102**:360–373.
8. Städtke H, Holtbecker R. Hyperbolic model for inhomogeneous two phase flow. *International Conference on Multiphase Flows*, University of Tsukuba, Japan, September 24–27, 1991.
9. Städtke H, Franchello G, Worth B. Toward a high resolution numerical simulation of transient two-phase flow. *Proceedings of the 3rd International Conference on Muliphase Flow*, Lyon, France, June 8–12, 1995.
10. Masella JM, Tran QH, Ferre D, Pauchon C. Transient simulation of two-phase flows in pipes. *International Journal of Multiphase Flow* 1998; **24**:739–755.
11. Masella JM, Faille I, Gallouet T. On an approximate Godunov scheme. *International Journal of Computational Fluid Dynamics* 1999; **12**:133–149.
12. Bedjaoui N, Sainsaulieu L. Analysis of a non-hyperbolic system modelling two-phase flows. 1. The effects of diffusion and relaxation. *Mathematical Methods in the Applied Sciences* 1997; **20**:783–803.
13. Bedjaoui N, Sainsaulieu L. Analysis of a non-hyperbolic system modelling two-phase flows: the effects of surface tension. *Mathematical Methods in the Applied Sciences* 1998; **21**:1519–1542.
14. Berger F, Colombeau JF. Numerical solution of one-pressure models in multifluid flows. *SIAM Journal on Numerical Analysis* 1995; **32**(4):1139–1154.
15. Tiselj I, Petelin S. High resolution shock capturing schemes for two-phase flow. *Proceedings of the ASME FED Summer Meeting*, 1996; 251–256.
16. Hwang YH. Upwind scheme for non-hyperbolic systems. *Journal of Computational Physics* 2003; **192**: 643–676.
17. Lee SJ, Chang KS, Kim KD. Pressure wave speeds from the characteristics of two fluids, two-phase hyperbolic equation system. *International Journal of Multiphase Flow* 1998; **24**:855–866.
18. Lee SJ, Chang KS, Kim KD. Surface tension effect in the two-fluid equation system. *International Journal of Heat and Mass Transfer* 1998; **41**:2821–2826.
19. Paillère H, Corre C, García-Cascales JR. On the extension of the AUSM+ scheme to compressible two-fluid models. *Computers and Fluids* 2003; **32**:891–916.
20. Pokharna H, Mori M, Ransom VH. Regularization of two phase flow models: a comparison of numerical and differential approaches. *Journal of Computational Physics* 1997; **134**:282–295.
21. Coquel F, El Amine K, Godlewski E, Perthame B, Raselet P. A numerical method using upwind schemes for the resolution of two phase flows. *Journal of Computational Physics* 1997; **136**:272–288.
22. García-Cascales JR. Conservative numerical schemes for unsteady 1D two-phase flow. *Ph.D. Thesis*, Universidad Politécnica de Valencia, Spain, 2001.
23. Bestion D. The physical closure laws in the CATHARE code. *Nuclear Engineering and Design* 1990; **124**: 229–245.

24. Saurel R, Abgrall R. A multiphase Godunov method for compressible multifluid and multiphase flows. *Journal of Computational Physics* 1999; **150**:425–467.
25. Corberán-Salvador JM, Gascón-Martínez Ll. TVD schemes for the calculation of flow in pipes of variable cross-section. *Mathematical and Computer Modelling* 1995; **21**:85–92.
26. Harten A. High resolution schemes for hyperbolic conservation laws. *Journal of Computational Physics* 1983; **49**:357–393.
27. Alouges F. Matrice signe et systemes hyperboliques. In *aspects theoriques et pratiques de la simulation numerique de quelques problemes physiques. Memorie d'habilitation*, Universite Paris-Sud, 1999.
28. Ghidaglia JM *et al.* An overview of the VFFC methods and tools for the simulation of two phase flows. *Technical Report*, *Report Note HT-33/99/005/A*, École Normal Supérieure de Cachan, 1999.
29. Toro EF. *Riemann Solvers and Numerical Methods for Fluid Dynamics*, *A Practical Introduction*. Springer: Berlin, 1997.
30. Hirsch C. *Numerical Computation of Internal and External Flows*, vol. 2. Wiley: New York, 1990.
31. Gascón-Martínez Ll, Corberán-Salvador JM. Construction of second-order TVD schemes for nonhomogeneous hyperbolic conservation laws. *Journal of Computational Physics* 2001; **171**:1–37.
32. Hewitt GF, Delhaye JM, Zuber N. *Numerical Benchmark Test*, volume 2. *Multiphase Science and Technology*. Wiley: New York, 1987.
33. Kumbaro A *et al*. Numerical benchmark problem specifications for two-fluid compressible flow solvers. *CEA Report*, 2002.
34. Toumi I, Kumbaro A. An approximate linearized Riemann solver for a two-fluid model. *Journal of Computational Physics* 1996; **124**:286–300.
35. Ghidaglia JM, Kumbaro A, Le Coq G. On the numerical solution to two fluid models via a cell centered finite volume method. *European Journal of Mechanics* 2001; **20**:841–867.
36. Toumi I. An upwind numerical method for two-fluid two-phase flow models. *Nuclear Science and Engineering* 1996; **123**:147–168.
37. Toumi I, Kumbaro A, Paillère H. Approximate Riemann solvers and flux vector splitting schemes for two-phase flow. *VKI Lecture Series 1999-03*, von Karmann Institute for Fluids Dynamics, 1999.
38. Tiselj I, Petelin S. Modelling of two-phase flow with second order accurate scheme. *Journal of Computational Physics* 1997; **136**:503–521.
39. Städtke H, Franchello G, Worth B, Graf U, Romstedt P, Kumbaro A, García-Cascales JR, Paillère H, Deconinck H, Ricchiuto M, Smith B, De Cachard F, Toro EF, Romenski E, Mimouni S. Advanced three-dimensional two-phase flow simulation tools for application to reactor safety. *Nuclear Engineering and Design* 2005; **235**:379–400.

